View metadata, citation and similar papers at core.ac.uk
brought to you by CORE
provided by Scientific Open-access Literature Archive and Repository

IL NUOVO CIMENTO Vol. 33 C, N. 1 Gennaio-Febbraio 2010
DOI 10.1393/ncc/i2010-10585-1

Colloquia: ICTT2009

# A Schrödinger-Poisson-Boltzmann system applied to the charge carrier transport in strained silicon

G. Toschkoff, G. Ossig, P. Lichtenberger, K. Zojer and F. Schürrer
*Graz University of Technology - Petersgasse 16, Graz, Austria*

(ricevuto il 30 Ottobre 2009; approvato il 5 Febbraio 2010; pubblicato online il 18 Marzo 2010)

**Summary.** — In this paper, a kinetic modeling of the electron transport inside a strained-silicon device structure is established. The reduced conduction band energy of a strained layer gives rise to a potential well structure, which may have a varying bottom energy. Electrons are introduced into the well by remote antimony doping, where they form a two-dimensional electron gas. Quantum-mechanical aspects are treated by using a self-consistent Schrödinger-Poisson block (subband model). To account for the transport properties of the strained-silicon device structure, an adapted semi-classical formulation of the Boltzmann transport equation is applied. This approach allows us to consistently include the relevant scattering mechanisms. The resulting coupled Schrödinger-Poisson-Boltzmann system is used for a phonon-limited mobility estimate.

PACS 73.23.-b – Electronic transport in mesoscopic systems.

## 1. – Introduction

The number of transistors on a memory chip or within a processor increases exponentially in time. Nowadays, this number approaches the tera scale. This has been achieved by a continuous reduction of the channel length of transistors. Gordon Moore, the founder of Intel, predicted this growth in 1965. But not only the downscaling is responsible for the incredible increase of the performance of electronic devices. Recently, scientists working in this field have pioneered a new form of silicon, which is called strained silicon [1]. In strained silicon, electrons experience less resistance and flow up to 70% faster, which boosts the chip speed up to 35%—and this without having to shrink the size of transistors.

There are still open questions concerning the mobility of charge carriers in strained silicon. Consequently, there exists a great challenge to develop appropriate methods to model the carrier transport in such materials [2, 3]. In this paper, a structure is treated which consists of strained silicon sandwiched between two SiGe layers. The lowered conduction band energy of the strained layer gives rise to a potential well structure. Electrons are introduced into the well by remote antimony doping, where they form a

© Società Italiana di Fisica

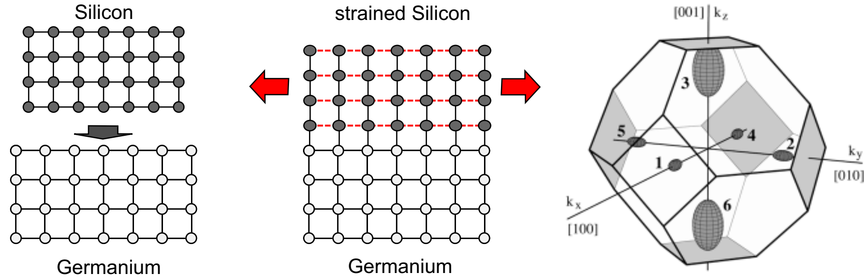


Fig. 1. – Left and middle plot: schematic representation of the creation of a strained-silicon layer. When silicon is grown on a germanium substrate, the silicon layer adapts the horizontal lattice spacing of germanium by imposing strain (indicated by the two horizontal arrows). Right plot: sketch of the six conduction band valleys in strained silicon in $k$-space. The six ellipsoidal shapes are isoenergetic surfaces. The energetically lowered valleys perpendicular to the interface have an enlarged isoenergetic surface (3 and 6). These bands are, therefore, higher occupied.

two-dimensional electron gas (2DEG). When actually building such devices, one cannot expect the potential well to have a constant bottom energy level [4]. With decreasing temperature, this potential modulation could lead to a capturing of the charge carriers. The scope of this work is to numerically simulate the influence of different parameters, especially a periodic modulation of the potential well, on the carrier mobility.

For the theoretical modeling, a coupled Schrödinger-Poisson-Boltzmann approach is used [5, 6]. Quantum-mechanical aspects are dealt with by means of a Schrödinger-Poisson block leading to a subband model. The backbone of our procedure is an adapted semi-classical formulation of the Boltzmann transport equation (BTE) describing the carrier movement in strained-silicon layers. The BTE allows us to consistently include the relevant scattering mechanisms without needing relaxation time approximations. A numerical solution algorithm is developed, based on a conservative finite-difference up-wind scheme. From the solution of the BTE, macroscopic quantities such as the current or the mobility are calculated as functions of different parameters.

## 2. – Physical modeling

For obtaining strained-silicon layers, one takes advantage of the natural tendency of atoms inside compounds to align with each other [7]. When silicon is deposited on top of a substrate with atoms spaced farther apart, the atoms in silicon must increase their spacing to line up with the atoms beneath, which means stretching or straining the silicon (fig. 1). A possible substrate material is germanium whose lattice constant is approximately 4% larger than that of silicon. Since this difference is very large, one uses a crystal consisting of a mixture of silicon and germanium. The lattice constant increases almost linearly with the germanium content [8].

In strained silicon, the band structure is dramatically changed [9]. Isotropic or hydrostatic strain is equally effective in all directions. This causes a shift of the energetic position of the 6-fold degenerated conduction band of silicon. Tensile strain in silicon layers leads to a splitting of the 6-fold degenerated band into a 4-fold degenerated in-plane and a 2-fold degenerated out-plane band. The six conduction band valleys in the first Brillouin zone of unstrained silicon are characterized by equivalent isoenergetic ellipsoidal surfaces; only their orientation is different. Tensile strain, however, causes

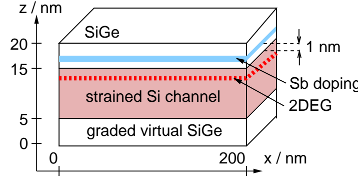


Fig. 2. – Real structure of a strained-silicon channel sandwiched between SiGe layers. A spacer separates the Si channel from the Sb doping layer, to ensure that the 2DEG do not encounter ionized impurities. We assume the device to be infinite perpendicular to the $(x, z)$-plane.

an energetic shift between the in- and out-plane valleys. The energetic lower out-plane valleys are much higher occupied with electrons, as indicated in fig. 1 by the larger size of the isoenergetic surfaces.

In thin silicon layers, we have a further band shift due to size quantization. Because of the different orientations of the in- and out-plane valleys and their direction-dependent effective masses, the size quantization is responsible for a different splitting of the in- and out-plane valleys into subbands. When dealing with confined electrons in strained silicon, we must, therefore, add the band shifts caused by confinement and strain.

The changed band structure in strained silicon leads to a substantial increase of the mobility. In thin layers of strained silicon, the confining potential forms a two-dimensional electron gas (2DEG), which means that the quasi-free motion of the electrons is restricted to a plane. The dominant occupation of the out-plane valleys and their vertical orientation (fig. 1) implies that only the lower transversal effective mass $m_t^* = 0.2\,m_0$ is responsible for the mobility of electrons in this plane, which, of course, increases their mobility. Consequently, the averaged effective mass of electrons moving in strained silicon is lower and the mobility correspondingly higher. Because of the high energy difference between the in- and out-plane valleys, phonon scattering between these valleys is suppressed, which leads to a further increase of the mobility.

In devices based on strained silicon, remote doping additionally increases the mobility. This fact is easily explained by considering a real structure with a channel of strained silicon, as shown in fig. 2. It consists of different layers: i) a so-called SiGe graduated virtual substrate, ii) followed by the transport channel of strained Si, where the electrons form a 2DEG close to the iii) spacer that separates the silicon channel from iv) a layer of SiGe partially doped with antimony. In such a structure, the electrons of the doping layer migrate to the transport region. Here they are trapped in the potential well caused by the changed band structure in strained silicon, as shown in the sketch of the band alignment of the channel, spacer and doping layer (fig. 3). Although the carriers are attracted by the electric field of the remote ionized donors they are restrained from going back by the potential well of height $\Delta E_s = 0.2\,\text{eV}$. They are squeezed against the wall and form a 2DEG. The separation of the 2DEG from the donors by the spacer avoids ionized impurity scattering and enhances the mobility as well. The charge of carriers and donors changes the confining potential to a typical triangular shape, as displayed in the right plot of fig. 3. All these important features must be included in the modeling of the carrier transport in such structures to determine the mobility of the electrons.

There exists an interesting hypothesis of Kasper and Werner [4] concerning the temperature-dependence of the mobility of electrons in strained-silicon channels. They observed under certain conditions a less pronounced decrease of the mobility with in-

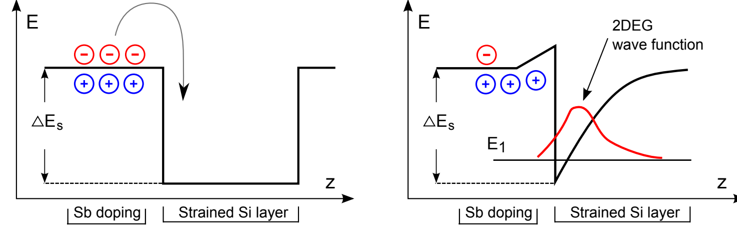


Fig. 3. – Modulation doping for a strained-silicon layer. The electrons leave the donors (left plot) and form a 2DEG near the interface, which alters the electrostatic potential (right plot) due to the charge of the electrons and ionized donors.

creasing temperature compared to the bulk case. Their idea to explain this observation is based on the assumption of a periodic modulation of the depth of the potential well, which confines the electron gas in a channel of strained silicon. The electrons are partially trapped in the valleys of the modulated well. Consequently, we assume in our modeling a sinusoidal variation of the depth of the confining potential.

## 3. – The Schrödinger-Boltzmann-Poisson system

We investigate the transport properties of electrons in a strained-silicon channel by means of a Schrödinger-Poisson block combined with a semi-classical Boltzmann equation. The connection of these equations to achieve a self-consistent solution for the steady state is represented in fig. 4. In the following, the physics behind this mathematical model is concisely explained.

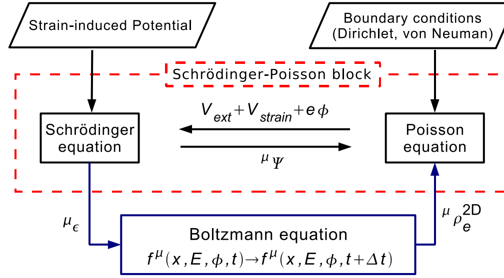


Fig. 4. – Schematic representation of the connection of the Schrödinger-Poisson block and the semi-classical Boltzmann equation. The self-consistent solution circle starts by solving the Poisson equation for the charge distribution of the donors and electrons. The resulting potential $\phi$ is added to the potential caused by the strain, $V_{\text{strain}}$, and the applied voltages, $V_{\text{ext}}$, and then, inserted into the Schrödinger equation to obtain the envelope wave functions $^{\mu}\psi$ and the eigenvalues $^{\mu}\epsilon$. Based on the updated charge distribution, the Poisson equation is solved again. This procedure is repeated until a self-consistent solution is obtained. The derivative of the eigenvalues with respect to the transport direction represents the effective force acting on the quasi-free moving electrons of the 2DEG. This force enters the advection operator of the Boltzmann equation. The solution of the Boltzmann equation after each time step is used to update the electron distribution along the channel $^{\mu}\rho_e^{2D}$ for performing the next discrete time step. This procedure must be continued until the steady state is reached.

**3**˙1. *The Schrödinger-Poisson block.* – The momenta of the electrons perpendicular to the plane of the 2DEG ($z$-direction in fig. 2) are quantized, which leads to electronic states characterized by subbands. The edges of the $\mu$-th subband are determined by the eigenvalues ${}^{\mu}\epsilon_i$ of the one-dimensional effective-mass Schrödinger equation

$$-\frac{\hbar^2}{2m_l^*}\frac{\partial^{\mu}\psi_i(z)}{\partial z} + V_i(z)^{\mu}\psi_i(z) = {}^{\mu}\epsilon_i{}^{\mu}\psi_i(z), \tag{1}$$

where ${}^{\mu}\psi_i(z)$ denotes the envelope wave function for electrons in subband $\mu$, $V_i(z)$ is the confining potential and $m_l^* = 0.92\,m_0$ the longitudinal effective mass of an electron in strained silicon. We solve the effective-mass Schrödinger equation at discrete positions $x_i$ along the channel. Since we assume a sinusoidal variation of the depth of the confining potential along the channel, we expect $x$-dependent eigenvalues. The potential

$$V_i(z) = V(x,z)\big|_{x=x_i} = [V_{\mathrm{ext}}(x) + V_{\mathrm{strain}}(z) + e\phi(x,z)]\big|_{x=x_i}$$

consists of an applied external potential $V_{\mathrm{ext}}(x)$, the potential $V_{\mathrm{strain}}(z)$ due to the band shift of the strained-silicon channel as well as the electrostatic potential $\phi(x,z)$ caused by the charge density of the ionized donors $\rho_{\mathrm{d}}(x,z)$ and the surface charge densities of the electrons in the 2DEG ${}^{\mu}\rho_e^{\mathrm{2D}}(x)$ of each subband; $e$ denotes the elementary charge.

The electrostatic potential $\phi(x,z)$ is calculated by the two-dimensional Poisson equation

$$\frac{\partial^2\phi(x,z)}{\partial x^2} + \frac{\partial^2\phi(x,z)}{\partial z^2} = -\frac{1}{\epsilon_0\epsilon_{\mathrm{r}}}\left[\rho_{\mathrm{d}}(x,z) + \sum_{\mu}{}^{\mu}\rho_e^{\mathrm{2D}}(x)|{}^{\mu}\psi_i(z)|^2\right]. \tag{2}$$

Here, $\epsilon_0$ stands for the permittivity of free space and $\epsilon_{\mathrm{r}}$ symbolizes the static dielectric constant. The spatial probability density $|{}^{\mu}\psi_i(z)|^2$ and the surface charge densities ${}^{\mu}\rho_e^{\mathrm{2D}}(x)$ of the electrons in the 2DEG determine the charge distribution within the channel of strained silicon. We apply Dirichlet boundary conditions at $x = 0$ and at $x = 200\,\mathrm{nm}$ as well as Neumann boundary conditions at $z = 0$ and at $z = 20\,\mathrm{nm}$.

The Schrödinger-Poisson block must be solved self-consistently resulting in a set of eigenvalues ${}^{\mu}\epsilon_i$ and eigenfunctions ${}^{\mu}\psi_i(z)$. For the numeric solution of the Schrödinger equation, the Shooting method combined with a Numerov scheme [10] is used. The derivatives in the Poisson equation are approximated be means of a finite-difference method. The resulting system of algebraic equations is treated by means of an interative Gauß-Seidl algorithm with successive overrelaxation.

**3**˙2. *The semi-classical Boltzmann equation.* – From a quasi-classical point of view, the set of eigenvalues obtained from the effective-mass Schrödinger equation can be interpreted as the potential energy of the electrons moving along the channel. Consequently, the spatial derivative of the eigenvalues with respect to the $x$-direction represents the effective force acting on the electrons. The corresponding distribution function for electrons in the $\mu$-th subband $f^{\mu}(x,E,\varphi,t)$, depending on the one-dimensional variable $x$ in real space and polar coordinates to represent the wave vector of the electrons in the plane of the 2DEG by $\boldsymbol{k} = (k_x(E,\varphi), k_y(E,\varphi))$, is governed by the semi-classical BTE

in conservative form [11]:

$$\begin{aligned}(3)\quad & \frac{\partial}{\partial t} f^\mu(x,E,\varphi,t) + \frac{\partial}{\partial x}\left[v(E,\varphi) f^\mu(x,E,\varphi,t)\right] \\ & + \frac{\partial}{\partial E}\left[F_k^\mu\,\Gamma(E)\frac{\hbar k(E)}{m_t^*} f^\mu(x,E,\varphi,t)\right] + \frac{\partial}{\partial \varphi}\left[F_\varphi^\mu\,\frac{1}{\hbar k(E)} f^\mu(x,E,\varphi,t)\right] = \frac{\partial C^\mu}{\partial t}\,.\end{aligned}$$

The energy of the electrons with respect to the band edge of the subband is denoted by $E$, and $\varphi$ is the angle between the wave vector and the $x$-direction. The distribution function $f^\mu(x,E,\varphi,t)$ is related to the surface charge density ${}^\mu\rho_e^{2\mathrm{D}}(x)$ by

$${}^\mu\rho_e^{2\mathrm{D}}(x) = e\int_0^\infty \mathrm{d}E \int_0^{2\pi} \mathrm{d}\varphi f^\mu(x,E,\varphi,t).$$

The non-parabolic dispersion relation $k(E) = \sqrt{2m_t^*\gamma(E)}/\hbar$ with $\gamma(E) = E(1+\alpha E)$, and $\alpha$ denoting the nonparabolicity factor, leads to the group velocity

$$(4)\qquad v(E,\varphi) = \frac{\hbar k(E)}{m_t^*}\Gamma(E)\cos(\varphi).$$

Here, we use the abbreviation $\Gamma(E) = [\partial\gamma(E)/\partial E]^{-1}$. The force acting on the electrons $(F_k^\mu, F_\varphi^\mu) = (F^\mu\cos(\varphi), F^\mu\sin(\varphi))$, which enters the advection operator of the Boltzmann equation, is determined by the derivative of the eigenvalues, $F^\mu(x) = e\,\mathrm{d}^\mu\epsilon(x)/\mathrm{d}x$. It should be noted that the eigenvalues are only given at discrete positions along the channel.

Scattering caused by acoustic phonons is the most important mechanism regarding the reduction of mobility in strained silicon. Therefore, to get an estimate for the phonon-limited carrier mobility, it suffices to focus on acoustic phonon scattering only. By taking into account intra- and inter-subband scattering, the collision operator of eq. (3) can be written as

$$\begin{aligned}(5)\quad \frac{\partial C^\mu}{\partial t} = & \sum_j \int_0^{2\pi} \mathrm{d}\varphi' \frac{2\pi}{\hbar}\frac{D_{\mathrm{ac}}^2 k_B T}{u_L^2\rho} I_{\mu j}^{\mathrm{ac}} \\ & \times\left[Z(E) f^j(x, E + {}^\mu\epsilon(x) - {}^j\epsilon(x), \varphi', t) - Z(E + {}^\mu\epsilon(x) - {}^j\epsilon(x)) f^\mu(x,E,\varphi,t)\right],\end{aligned}$$

by using Fermi's Golden Rule. Here, ${}^\mu\epsilon$ and ${}^j\epsilon$ denote the subband energy of initial and final state, respectively, and $T$ the temperature. The form factor is given by $I_{\mu j}^{\mathrm{ac}} = \int_{-\infty}^{\infty} \mathrm{d}z\,[{}^\mu\psi^*(z){}^j\psi(z)]^2$, and the density of states reads $Z = m_t^*\partial_E\gamma(E)/2(\pi\hbar)^2$. In the following simulations, we use the acoustic deformation potential $D_{\mathrm{ac}}^2 = 12\,\mathrm{eV}$, the longitudinal speed of sound $u_L = 9.37\cdot 10^{12}\,\mathrm{nm\,s^{-1}}$ and the mass density of silicon $\rho = 2330\,\mathrm{kg\,m^{-3}}$.

The advection operator of the BTE is approximated by an upwind finite-difference scheme and the collision operator by the midpoint rule, which is of second-order accuracy. The time integration of the resulting system of ODE is performed by applying an explicit Euler time-step scheme and by imposing periodic boundary conditions. After each time step, the solution of the Boltzmann equation is used to update the electron distribution along the channel. Then, another self-consistant solution of the Schrödinger-Poisson block is evaluated, which provides us with updated eigenvalues and eigenfunctions for

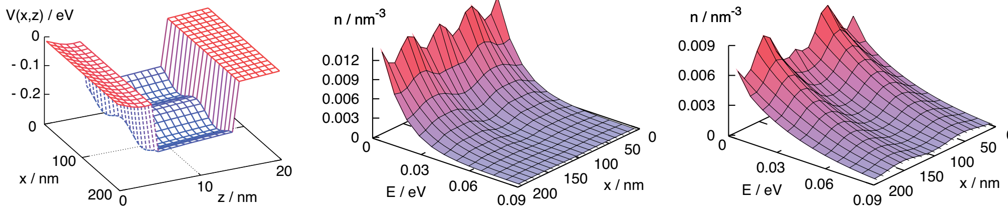


Fig. 5. – Potential $V(x,z)$ in the channel of strained Si and neighbouring zones for an applied field strength of $0.05\,\mathrm{kV\,cm^{-1}}$ at steady state and $A_{\mathrm{mod}} = 0.05\,\mathrm{eV}$ (left). Time evolution of the electron density $n(x,E)$ at $t = 10^{-13}\,\mathrm{s}$ (middle) and at $t = 10^{-12}\,\mathrm{s}$ (right) close to the steady state at room temperature and for an applied field strength of $0.05\,\mathrm{kV\,cm^{-1}}$.

performing the next time step by solving the BTE (fig. 4). This procedure is continued until the steady state is reached.

## 4. – Simulation results and discussion

In the performed simulations, we take into account two subbands for the electronic states in strained silicon. We assumed a sinusoidal potential modulation with a period of 100 nm and consider two different modulation amplitudes $A_{\mathrm{mod}} = 0.0005\,\mathrm{eV}$ and $A_{\mathrm{mod}} = 0.05\,\mathrm{eV}$. The left plot in fig. 5 displays the resulting potential $V(x,z)$ at steady state. Starting from a homogeneous Fermi-Dirac distribution of the electrons in the channel, the temporal evolution of the electron density $n(x,E) = \sum_\mu \int_0^{2\pi} \mathrm{d}\varphi f^\mu(x,E,\varphi,t)$ at two instants of time is shown in the middle and left plot of fig. 5. It can be seen that the mean electron energy increases temporarily and that the carriers gather at the positions of the potential minima.

The electron mobility depends on several parameters. We study the influence of the most important ones, namely that of the temperature, the electric field strength and the amplitude of the sinusoidal potential modulation. In the case of a vanishing modulation, the obtained mobilities are in good agreement with literature values for strained silicon without considering a modulation [12]. Interesting results of our simulations are depicted in fig. 6. Here, we have plotted the mobility $\mu = v_x(x)/E_x$, where $E_x$ denotes the external

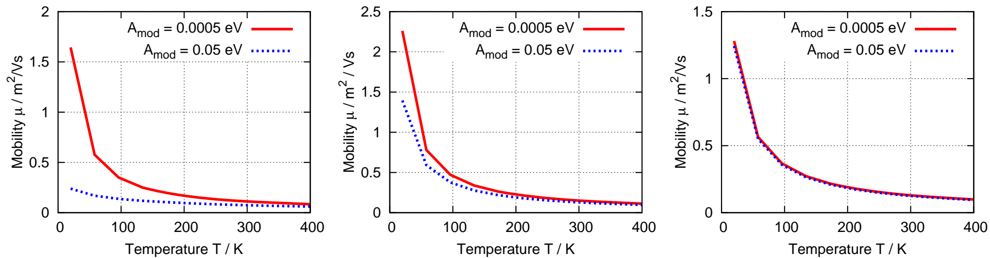


Fig. 6. – Electron mobility $\mu$ as a function of temperature $T$ for an applied electric field $V_{\mathrm{f}} = 0.0005\,\mathrm{kVcm^{-1}}$ (left), $V_{\mathrm{f}} = 0.05\,\mathrm{kVcm^{-1}}$ (middle), $V_{\mathrm{f}} = 5\,\mathrm{kVcm^{-1}}$ (right), and an electron sheet density $\rho_{\mathrm{e}}^{\mathrm{2D}} = 1 \cdot 10^{-3}\,\mathrm{nm^{-2}}$. The current is $i = 7.7 \cdot 10^{-13}\,\mathrm{C\,nm^{-2}}$ (left), $i = 7.7 \cdot 10^{-11}\,\mathrm{C\,nm^{-2}}$, (middle), $i = 7.6 \cdot 10^{-9}\,\mathrm{C\,nm^{-2}}$ (right).

applied electric field strength and $v_x(x)$ the drift velocity of the electrons in $x$-direction determined by the distribution functions of electrons in the subbands $f^\mu(x, E, \varphi, t)$ and the group velocities of the electrons due to eq. (4). It is well known that acoustic phonon scattering decreases the mobility with rising temperature. The left and the middle plot in (fig. 6) reveal that the reduction of the mobility is less pronounced in the case of a high modulation amplitude of the sinusoidal potential well. Furthermore, it can be seen that the influence on the mobility of keeping the electrons in the valleys of the potential well decreases with rising temperature. The observation that the effect of the sinusoidal potential modulation on the mobility vanishes at high electric field strengths (right plot in fig. 6), can be explained by the fact that the averaged negative slope of the potential well in $x$-direction increases with rising field strength. This means, there exists no longer a positive slope at any position of the sinusoidal variation of the depth of the potential well. Increasing modulation amplitudes obviously raises the effect of keeping the electrons in the potential valleys, especially at lower temperatures.

## 5. – Conclusion

This paper presents a Schrödinger-Poisson-Boltzmann system to simulate the electron transport in strained-silicon device structures. The chosen approach takes into account the band shift in silicon due to strain, the effect of remote doping, the formation of a two-dimensional electron gas in the channel as well as the most important phonon intra- and inter-subband scattering mechanism in silicon. The performed simulations focus on the temperature- and electric-field–dependence of the electron mobility by considering a sinusoidal modulation of the depth of the confining potential in the channel of strained silicon. Most important is the finding that there exists remarkable influence of the modulation depth on the temperature and field dependence of the mobility, which approves the hypothesis of Kasper and Werner [4].

* * *

The authors are indebted to E. Kasper, Institut für Halbleitertechnik, Universität Stuttgart, Germany, for drawing their attention to the investigated problem.

REFERENCES

[1] Minjoo L. L., Fitzgerald E. A., Bulsara M. T., Currie M. T. and Lochtefeled A., *J. Appl. Phys.*, **97** (2005) 011101.
[2] Toshishige Y., Miyata H., Zhou J.-R. and Ferry D. K., *Phys. Rev. B*, **49** (1994) 1875.
[3] Dziekan T., Zahn P., Meded V. and Mirbt S., *Phys. Rev. B*, **75** (2007) 195213.
[4] Kasper E. and Werner J., Institut für Halbleitertechnik, Universität Stuttgart, private communications.
[5] Ertler C. and Schürrer F., *J. Comput. Electron.*, **5** (2006) 15.
[6] Ossig G. and Schürrer F., *Comput. Electron.*, **7** (2008) 367.
[7] Perova T. S., Lyutovich K., Kasper E., Waldron A., Oehme M. and Moore R. A., *Mater. Sci. Eng. B*, **135** (2006) 192.
[8] Schäffler F., *Semicond. Sci. Tech.*, **12** (2008) 12.
[9] Kasper E. and Paul D. J., *Silicon Quantum Integrated Circuits: Silicon-Germanium Heterostructure Devices: Basis and Realizations* (Springer, Berlin) 2005.
[10] Quiroz González J. L. M. and Thompson D., *Comput. Phys.*, **11** (1997) 515.
[11] Galler M., *Multigroup Equations for the Description of the Particle Transport in Semiconductors* (World Scientific, Singapore) 2005.
[12] Takagi S. I., Hoyt J. L., Welser J. J and Gibbons J. F., *J. Appl. Phys.*, **80** (1996) 3.